Journal of Micromechanics and Microengineering

PAPER • OPEN ACCESS

Thermal analysis of the ceramic material and evaluation of the bonding behavior of silicon-ceramic composite substrates

To cite this article: Laura Mohr-Weidenfeller *et al* 2022 *J. Micromech. Microeng.* **32** 105004

View the article online for updates and enhancements.

You may also like

- Development of a Novel Low Temperature Co-Fired Ceramics System Composed of Two Different Co-Firable Low Temperature Co-Fired Ceramics Materials
Takaki Murata, Satoshi Ohga and Yasutaka Sugimoto

- Modelling of sawtooth-induced fast ion transport in positive and negative triangularity in TCV
Matteo Vallar, Mario Podestà, Marcelo Baquero-Ruiz et al.

- Mechanical quality factor enhancement in a silicon micromechanical resonator by low-damage process using neutral beam etching technology
Nguyen Van Toan, Tomohiro Kubota, Halubai Sekhar et al.

This content was downloaded from IP address 202.8.112.141 on 08/06/2023 at 07:39

OPEN ACCESS
IOP Publishing
Journal of Micromechanics and Microengineering
J. Micromech. Microeng. **32** (2022) 105004 (9pp)
https://doi.org/10.1088/1361-6439/ac8686

Thermal analysis of the ceramic material and evaluation of the bonding behavior of silicon-ceramic composite substrates

Laura Mohr-Weidenfeller[1], **Cathleen Kleinholz**[2], **Björn Müller**[2], **Sebastian Gropp**[1], **Sarah Günther-Müller**[1], **Michael Fischer**[2], **Jens Müller**[2] and **Steffen Strehle**[1,*]

[1] Technische Universität Ilmenau, Institute of Micro- and Nanotechnologies IMN MacroNano®, Microsystems Technology Group, Ilmenau, Germany
[2] Technische Universität Ilmenau, Electronics Technology Group, Ilmenau, Germany

E-mail: steffen.strehle@tu-ilmenau.de

Received 27 April 2022, revised 23 July 2022
Accepted for publication 3 August 2022
Published 19 August 2022

Abstract
Thermal bonding of silicon and low-temperature cofired ceramics (LTCC) at sintering temperatures of 900 °C represents currently the standard process in silicon-ceramic composite (SiCer) substrate fabrication. We analyse the thermal behavior of the LTCC using thermogravimetric analysis, differential scanning calorimetry and laser flash analysis. The thermal decomposition could be identified with a mass loss of 24% in the temperature range up to 1000 °C what influences the thermal diffusivity with values from about 0.19 $mm^2\ s^{-1}$ before thermal treatment to below 0.10 $mm^2\ s^{-1}$ after thermal treatment. A specific heat capacity of 1–2 J $(g \cdot K)^{-1}$ is calculated. Further, an influence of low-temperature lamination of the LTCC seems to have an influence on the thermal behaviour. The sintering process was investigated with temperatures of 550 °C, 730 °C and 900 °C, applied pressures of 12.2 kPa and 6.1 kPa and intermediate wetting layers of TiO_2 (normal deposition and oblique angle deposition). Optical observations, ultrasonic and scanning electron microscopy, and pull-tests are used to compare the properties of the sintered SiCer substrates. Whereas the sintering temperature has an obvious impact on the sintering behaviour of the LTCC, a direct conclusion of parameter variation on the bonding result was not observed.

Keywords: SiCer, sintering, bonding, thermal analysis

(Some figures may appear in colour only in the online journal)

* Author to whom any correspondence should be addressed.

Original content from this work may be used under the terms of the Creative Commons Attribution 4.0 licence. Any further distribution of this work must maintain attribution to the author(s) and the title of the work, journal citation and DOI.

1. Introduction

Semiconductors and ceramics are crucial substrate material classes in the field of microsystems and electronics. Conventional microtechnologies are mainly suited for standard substrate materials such as silicon wafers enabling processes like photo- and e-beam lithography, chemical and physical vapor deposition, and wet and dry etching processes [1]. Ceramic substrates like low-temperature cofired ceramics (LTCC) require in contrast an own technology set for microfabrication comprising thick film manufacturing, e.g. pattern punching, laser cutting and screen-printing [2]. LTCC tapes enable a manufacturing of functional devices at relatively low cost with small footprint by processing each single layer followed by their stacking prior to a thermal sintering process. In this way, passive components, wiring and vias can be effectively realized [2]. Especially the dielectric properties of the LTCC render it as a superior material for high frequency applications [2]. Obviously, both materials, silicon and LTCC, exhibit unique advantages but partly in contrary fields of application. Hence, a combined use of silicon and ceramics as a single substrate or at least as a common material platform is intriguing and creates new possibilities for advanced microsystems that can cope with complex application scenarios.

Thermal bonding of silicon and LTCC at sintering temperatures of 900 °C represents currently the standard process in silicon-ceramic composite (SiCer) substrate fabrication [3]. A quasi-monolithic SiCer substrate can be made by co-sintering of LTCC and silicon while basic functionalities regarding electrical connections from LTCC to silicon can be implemented using through silicon vias [4, 5]. The LTCC material, originally bondable ceramic tape (BCT), was developed for anodic bonding of silicon and LTCC and offers an accordingly adapted thermal coefficient of expansion to silicon [4]. To assure improved compatibility to alkaline sensitive silicon processes, another LTCC generation with alkaline-free glass components was therefore recently introduced [2, 4]. Due to the initially required relatively high sintering pressures in the range of 800 kPa, investigations on wetting promoting layers were triggered to lower the required pressure. Intermediate TiO_2 thin layers appear, for instance, to reduce the needed sintering pressure dramatically [6] leading the so-called pressure-assisted sintering with pressure of as low as 3 kPa [3]. The benefits of SiCer substrates are, for instance, demonstrated in radio frequency micro-electro-mechanical systems (RF-MEMS) applications [2, 7].

The sintering process is within the SiCer substrate fabrication one of the critical key steps. Joining both materials reproducibly and with high yield must be therefore based on an understanding of the underlying mechanisms. Thus, knowledge about the required temperature profile during sintering as well as about the overall thermal material parameters and behavior is essential in this context. Silicon alone is a rather well-known material. The thermal behavior of the used LTCC is, however, still quite unknown, which is in particular true for the combined sintering of silicon and ceramic material. We address this issue with thermogravimetric analysis (TGA), differential scanning calorimetry (DSC) and laser flash analysis (LFA) measurements of LTCC material. The recorded data clearly show the outgassing of solvents and binders. Furthermore, the heat capacity and thermal diffusivity can be calculated based on the performed thermal analysis. Sintering at different temperatures is examined under consideration of the glass transition temperatures of the LTCC components. In addition to the thermal analysis, the impact of the sintering pressure and of an intermediate TiO_2 layer are studied. The latter includes a modification of the TiO_2 thin film morphology by employing oblique angle deposition to yield oblique TiO_2 nanorod assemblies. These investigations are evaluated by optical observations, ultrasonic microscopy, scanning electron microscopy (SEM) analysis and by means of pull-tests.

2. SiCer fabrication process

For the SiCer fabrication process, a customized LTCC tape called BCT type 6 (developed by Fraunhofer Institute for Ceramic Technologies and Systems (IKTS), Hermsdorf, Germany) was utilized. Aluminoborosilicate glass (AF32 and AF45, Schott, Mainz, Germany) and magnesium aluminum silicate (Cordierit, IKTS, Hermsdorf, Germany) represent the solid tape components. Polyoxyethylene nonylphenyl ether phosphate (Rhodafac RE 610, Solvay, Brussels, Belgium) is added as dispersant and polyvinyl butyral (B98 and B79 Butvar, Eastman Chemical, Kingsport, Tennessee, USA) as well as diisononyl phthalate (DINP, Liquichem, Hamburg, Germany) as plasticizers.

The BCT tapes are laminated to create double tapes that are laminated again to a BCT stack, that is finally laser cut into 2 inch wafer contours. If more than just a plain non-patterned substrate is required, the tapes can be pre-processed by punching, laser cutting and screen-printing before sintering to add functional components and interconnects. For the silicon component, conventional single-crystalline silicon 2 inch wafers with a thickness of 300 μm and a total thickness variation of $\pm$10 μm (Siegert Wafer GmbH, Aachen, Germany) are used.

A thin TiO_2 wetting layer of about 50 nm is deposited by, e.g. sputter deposition and dry oxidation, onto the wafer side that will be finally in contact with LTCC. The sputtering of the thin titanium layer does not measurably change the initial roughness of the silicon wafer and is negligible compared to the roughness of the flexible, almost film-like LTCC greentape. Before sintering the LTCC, it has a roughness of less than 10 μm. Thus, the flexible LTCC fits perfectly to the Si wafer during lamination. The roughness (Ra) of the LTCC decreases during the sintering process since the glass in the LTCC matrix melts and wets the titanium surface. After independent pre-processing, the LTCC and the silicon wafer are stacked and aligned. The stack is then laminated in an isostatic press at 82 °C for 15 min with a maximum pressure of 21 MPa, which includes a pre-heating of 4 min. The final sintering is subsequently realized at temperatures of up to 900 °C, which yields a quasi-monolithic SiCer substrate. The individual steps of the previously described fabrication process are depicted in figure 1.

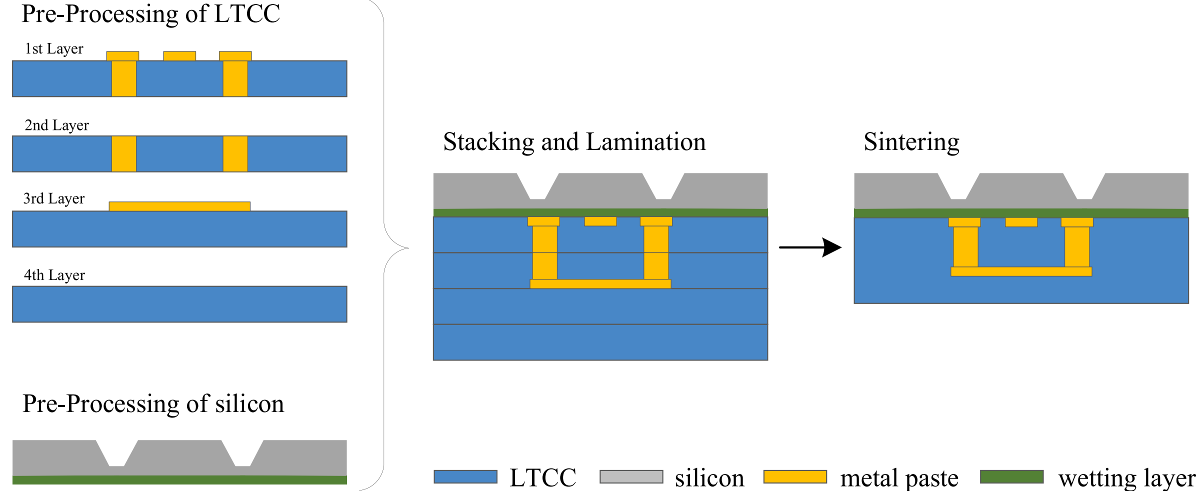

Figure 1. Schematic illustration of a representative SiCer fabrication process. Simultaneous and independent pre-processing of LTCC and silicon, followed by stacking and lamination for a first arrangement of both wafers. Subsequently, the material stacked material is sintered to yield a quasi-monolithic SiCer substrate.

3. Methodology

3.1. Thermal analysis of LTCC

TGA of LTCC in unlaminated and laminated state was realized by using a TGA Q5000 IR (TA Instruments, New Castle, DE, USA). The analysis was carried out in the temperature range of 20 °C–1000 °C in the so-called high-resolution mode with a heating rate of 10 K min^{-1} under nitrogen atmosphere. A subsequent second measurement run was conducted to ensure that the first measurement covers all occurring mass losses in the selected temperature regime. For reasons of comparability with the sintering temperatures typically specified in °C, temperatures for thermal analysis are also given here in °C instead of K.

Using a differential scanning calorimeter DSC 204 F1 2920 (Netzsch-Gerätebau GmbH, Selb, Germany), the specific heat capacities of LTCC in unlaminated state and being laminated to a double layer were measured from 40 °C to 600 °C using a heating rate of 10 K min^{-1} and a nitrogen atmosphere. The DSC tool was calibrated in this temperature range using sapphire (Al_2O_3) as standard sample following DIN 51007. The accuracy of the measurements is estimated to be better than 3%.

The temperature-dependent thermal diffusivity $\alpha(T)$, which correlates with the thermal conductivity $\lambda(T)$, specific heat capacity $c_p(T)$, and specific density $\rho(T)$ by the relation $\alpha = \lambda/(c_p \cdot \rho)$, was investigated in a laser flash apparatus (LFA 427, Netzsch-Gerätebau GmbH, Selb, Germany) from 20 °C to 500 °C under helium atmosphere. A laminated double layer of LTCC was laser-cut into circles with a diameter of 1 inch. The sample was covered by a thin graphite layer to ensure sufficient absorption of the laser light and to prevent any surface deterioration by the impact of the laser pulse. Pure LTCC tapes without vias or screen printing pastes were used for all analyses.

3.2. Interface modifications

To analyze the impact of the aforementioned interface modifications on the bonding quality of SiCer substrates, silicon wafers were either used without any intermediate layer or were coated with a 32 nm thick layer of Ti using sputter deposition (Ardenne CS400, VON ARDENNE GmbH, Dresden, Germany). After dry oxidation (Tempress Junior, Tempress Systems, Vaasen, Netherlands), a 50 nm thick TiO_2 layer is obtained. Based on previous reports [6] and the known dependency of the wetting behavior on surface roughness [8], titanium was furthermore, deposited by electron beam evaporation at an oblique angle (OAD: oblique angle deposition), which leads to oblique titanium nanorods [9]. SEM images of the deposited titanium nanorods are shown in figures 2(a) and (b). The purpose of these nanorods is the utilization of titanium not only as a wetting layer but also as a nanostructured compliant layer [10] to reduce residual stresses originating from the slight remaining mismatch of thermal expansion coefficient between the LTCC, the titanium film and the silicon. In addition, the nanorods should be better able to compensate asperities at the silicon-LTCC interface, supporting lower sintering pressures [6]. The resulting titanium nanorods were not intentionally oxidized but a native oxide can be assumed.

3.3. Sintering experiments

The pressure assisted sintering of the investigated SiCer substrates was performed at pressures of 6.1 kPa and 12.2 kPa to investigate the influence of different applied pressures on the bonding interface. The pressure is applied via static weights, which are uniformly applied to the entire surface of the substrate. Due to the glass transition temperatures of the glass additives in LTCC, end temperatures of 550 °C and 730 °C were chosen as maximum sintering temperatures in addition

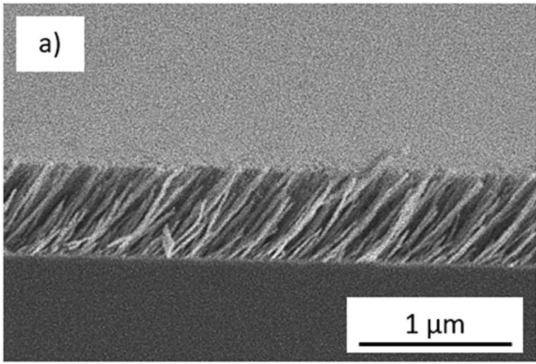

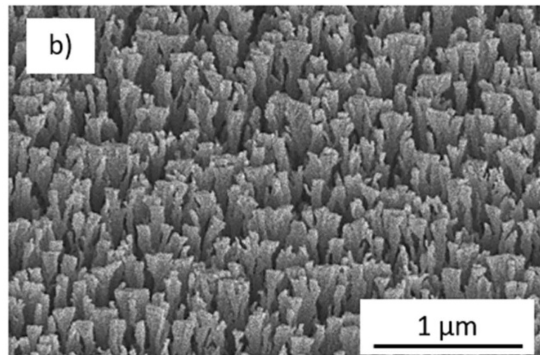

Figure 2. (a) SEM cross sectional and (b) top view of the silicon substrate covered by titanium nanorods obtained by oblique angle deposition.

Table 1. Parameters regarding sintering pressure, sintering temperature and interface modification and their assignment to the substrate label or experiment S1–S7 (OAD).

	S1	S2	S3	S4	S5	S6	S7
Pressure (kPa)	12.2	6.1	12.2	12.2	6.1	12.2	12.2
Temperature (°C)	900	900	900	900	900	550	730
Interface	TiO_2	TiO_2	Ti (OAD)	—	—	TiO_2	TiO_2

to the standard sintering temperature of 900 °C. An overview of the conducted experiments is shown in table 1, which are denoted by the substrate label S1–S7 in the following.

The preparation of the substrates S1–S7 were done following the description in section 2 without any punching or screen printing. Thus, the resulting ceramic side is pure LTCC without any vias or applied metal pastes. In total, three laminated double tapes of LTCC with a total thickness of about 780 μm were stacked again laminated with the silicon wafer prior to sintering. The lamination is conducted in an isostatic press at 82 °C for 15 min with a maximum pressure of 21 MPa, which includes a pre-heating of 4 min. The silicon wafer is either used without any treatments or with pre-processing of the interface according to table 1. The slight pressure during sintering is applied by loading sintering plates on the stack.

3.4. Analysis of the bonding behavior

The substrates were inspected after sintering optically by the bare eye and by using an optical scanner to assess the overall color of the ceramic surface, while the homogeneity of the SiCer interface was evaluated by images obtained by ultrasonic microscopy (Nordson Corporation, Westlake, USA). The interface bond strength was quantitatively analyzed by using a pull-test method. Samples were prepared in this regard by dicing the substrates into 10 × 10 mm^2 chips. The chips were glued onto aluminum sample holders employing an epoxy-based glue (2AIF, Innovative Klebetechnik Zimmermann, Jena, Germany). Subsequent curing at 180 °C was carried out for 15 min. The pulling tests were realized using an inspekt table 20-1 (Hegewald & Peschke Meß- und Prüftechnik GmbH, Nossen, Germany) pulling tool. The abort criterion for breaking was set to a force of 95% of the maximum pulling force $F_{\max}$.

4. Results and discussion

4.1. Thermal analysis of LTCC

As shown in figure 3(a), TGA measurements indicate a significant mass loss of the ceramic material during the first temperature cycle for both, unlaminated (black dotted line) and laminated (red dotted line) LTCC. The mass loss of unlaminated LTCC, following the first part of the curve, appears up to about 200 °C and is most likely caused by the evaporation of the solvents toluene (boiling point 111 °C [11]) and cyclohexanone (156 °C [12]) both of which are contained in LTCC. Between 200 °C and about 500 °C another mass loss occurs that sums up with the first mass loss to a total mass loss of about 24%, which can be clearly divided into two separate sections. One from 200 °C to 300 °C with about 10% mass loss and one from 300 °C to 500 °C with about 12% mass loss. Both sections can be linked to the binder polyvinylbutyral [13, 14]. The first section should originate from oxidative decomposition of the binder. However, as the measurement was carried out in an inert gas atmosphere, the second mass loss cannot be caused by oxidative decomposition and therefore, a pyrolytic decomposition of solvents and binders must be assumed. Above temperatures of about 500 °C, the sample weight remains almost constant. For laminated LTCC the total mass loss is the same, however an additional mass loss can be observed compared to unlaminated LTCC. The first mass loss occurs in the same range as for unlaminated LTCC, whilst the second mass loss takes place at temperatures between 300 °C and 400 °C. The third mass loss is shifted to slightly higher temperatures compared to unlaminated LTCC and occurs at temperatures between 400 °C and 600 °C. As shown, the first significant drop in the mass loss between 200 °C and 280 °C shows only slight differences between laminated and

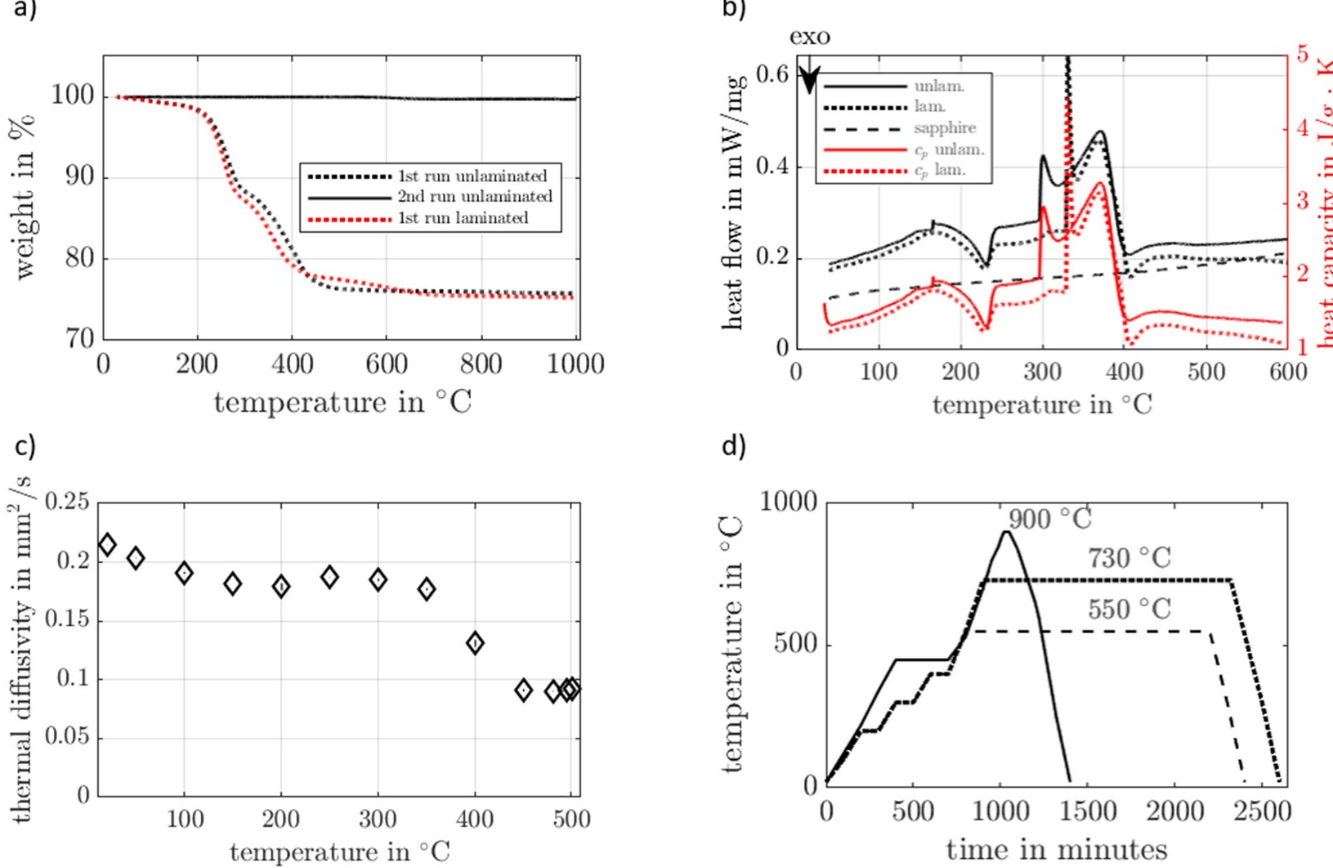

Figure 3. (a) Two consecutive TGA measurements of the LTCC green tape in unlaminated state, which show the percentage weight loss during the first heating run (dotted line) and the second heating run (solid line) and TGA measurement after lamination process for the first heating (red dotted line). The result for the second heating run in case of laminated LTCC is not visible due to overlap with the second heating of unlaminated LTCC. (b) DSC measurement data of unlaminated (black solid line) and laminated LTCC (black dotted line) as well as of the sapphire reference sample (black dashed line). Specific heat capacity c_P of unlaminated (red solid line) and laminated LTCC (red dotted line) was calculated from these data. (c) Thermal diffusivity given by LFA measurements of a laminated double layer LTCC. The data show the mean value of three measurements per temperature. (d) Temperature profile for the standard sintering process of SiCer substrates with a maximum temperature of 900 °C (solid line), adapted heating rate and times at temperature for gas emission of organic components and subsequent heating up to maximum temperature of 550 °C (dashed line) and 730 °C (dotted line).

unlaminated material, while the second significant mass loss between 280 °C and 400 °C for the laminated material and 280 °C and 420 °C for the unlaminated material is slightly shifted to lower temperatures for the laminated material. While the mass loss for the unlaminated material stops at around 500 °C the laminated material shows a further mass loss of only around 1% up to a temperature of 600 °C. This behavior is expectable. Organic materials are usually almost entirely decomposed during a temperature increase up to 450 °C. In the case of the laminated material, the organic binders close to cuts of the TGA samples can more easily escape from the material than the binder in the ceramics. Thus, the mass loss in the laminated materials appears at slightly lower temperatures compared to the unlaminated material. Finally, the binder between the two laminate layers has longer diffusion paths, which leads to a delayed decomposition and therefore to a delayed mass loss up to 600 °C. However, it must be kept in mind that this delayed mass loss concerns only 1% of the entire mass loss. In support, a second measurement (solid line) or temperature cycle shows no further significant weight loss with respect to the measuring uncertainty. In particular, no mass changes are visible in the first run for temperatures above 800 °C. Thus, also no mass loss can be expected in the second run. Finally, only a mass increase in the second run could appear due to oxidation of the material. That this is not the case and demonstrates the completion of the ceramic sintering process.

The results of the DSC and accordingly calculated specific heat capacities are shown in figure 3(b). For each sample, three heating cycles were recorded. However, the second and third heating cycle did not exhibit any effect on the measured heat flow and thus, indicate that all thermally induced material chances are mainly completed during the first run. In unlaminated state, there is a minute endothermic peak at about 170 °C that does not occur for laminated BCT. The underlying process seems to be addressed either at 170 °C or at lamination at low temperatures with applied pressure. An exothermic peak at 230 °C can be observed for both samples and is attributed here to cold crystallization processes in the binder as well as the plasticizer both contained in LTCC. At 300 °C, unlaminated

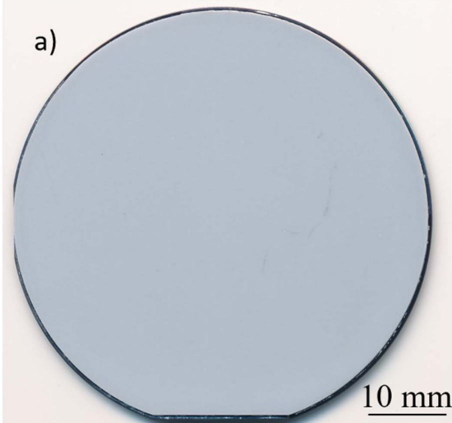

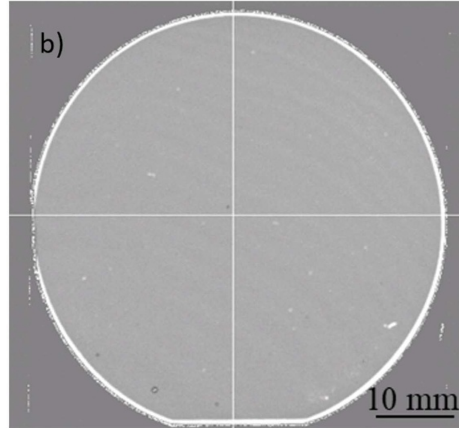

Figure 4. (a) Optical and (b) sonographic scan of a homogeneously bonded SiCer substrate substrate (experiment S4) after sintering with view to the ceramic side in case of (a).

LTCC shows a highly pronounced endothermic peak corresponding with the second weight loss in TGA measurements, followed by a very broad second endothermic peak at around 370 °C, whereas the laminated LTCC shows a very slight endothermic peak at 310 °C, followed by a highly pronounced peak at around 330 °C and a similar behavior as unlaminated LTCC at temperatures of 370 °C. For temperatures higher than 400 °C, no impact of thermal treatment within the investigated temperature range can be observed. The sample weight after DSC measurements was reduced by about 24%, which is in adequate agreement with the TGA measurements.

The shift and the sharpness of the endothermic peak from 300 °C in case of unlaminated LTCC to 330 °C in laminated LTCC can be attributed to a higher grade of crystallinity in the polymeric binder due to pressure and temperature during lamination, which leads to a higher melting temperature. The specific heat capacity calculated from the DSC measurement data with respect to the sapphire reference shows values from 1 to 2 J $(g \cdot K)^{-1}$. In the temperature ranges where endothermic or exothermic peaks occur, the calculated specific heat capacity is not reliable due to underlying phase changes or other reactions.

The results from LFA measurements are shown in figure 3(c). The curves of the detector signals after the laser pulse showed the best fit with the applied Cowan model [15, 16]. Shown measurement values represent the average values of three individual measurements. The accuracy of this method is assumed to be better than 3%. The specific density of LTCC was calculated to be 1.64 g cm^{-3} by using the geometric and the weight data, so the resulting accuracy of the thermal diffusivity is about 5%. The thermal diffusivity is higher than 0.2 mm^2 s^{-1} for temperatures below 50 °C. For temperatures between 100 °C and 350 °C the diffusivity is about 0.18–0.19 mm^2 s^{-1}, whereas it decreases for higher temperatures to values below 0.10 mm^2 s^{-1}. For glass, the thermal diffusivity is given with values from 0.56 to 1.70 mm^2 s^{-1} and for pressed ceramic powders with values about 0.1–0.2 mm^2 s^{-1} in literature [17–19]. The measured diffusivity of LTCC is comparable to these data. In comparison to the DSC data, a correlation between the endothermic peaks at about 330 °C and 370 °C and the decrease of thermal diffusivity can be assumed.

The results of the thermal analysis of the BCT tape suggest an adaption of the standard sintering profile. For sintering temperature profiles, the measurement results of the first TGA run is considered as relevant. The rapid weight loss of almost 24% takes place in the temperature range from 200 °C to 500 °C. An adaptation of the temperature profile for the sintering process is therefore suggested. A first holding temperature should therefore be shifted to 200 °C instead of 450 °C. This allows a slow outgassing of the solvents. This holding temperature should be followed by a slower temperature increase up to 500 °C with additional holding temperatures. If possible, a holding temperature at approx. 300 °C should also be provided due to the observed first endothermic peak in the DSC curves of the unlaminated sample. For the laminated sample the holding temperature should be around 330 °C. At this temperature, both the second mass loss in the TGA measurement and the endothermic peak in the DSC curve can be seen. The temperature profiles used in this work are shown in figure 3(d).

4.2. Sintering results and bonding behavior

The processed SiCer substrates S1–S7 (see table 1) were evaluated after the sintering process by optical inspection and by ultrasonic microscopy. Results of the optical inspection of substrate S4 are shown as an example for a homogeneously bonded SiCer substrate. The according optical scan is shown in figure 4(a), while the result of the sonographic scan is shown in figure 4(b). Optically, the overall color of the ceramic surface is homogeneous and no debonding between silicon and ceramic is obviously visible. The homogeneous gray coloring of the sonographic scan confirms a homogeneous bonding at the silicon-ceramic-interface.

Even though the sonographic scan shows a homogeneous bonding interface, the bond strengths (see figures 5(a) and (b)) vary considerably. The sample positions are numbered, as shown in figure 5(b) inset, for better assignment of the results.

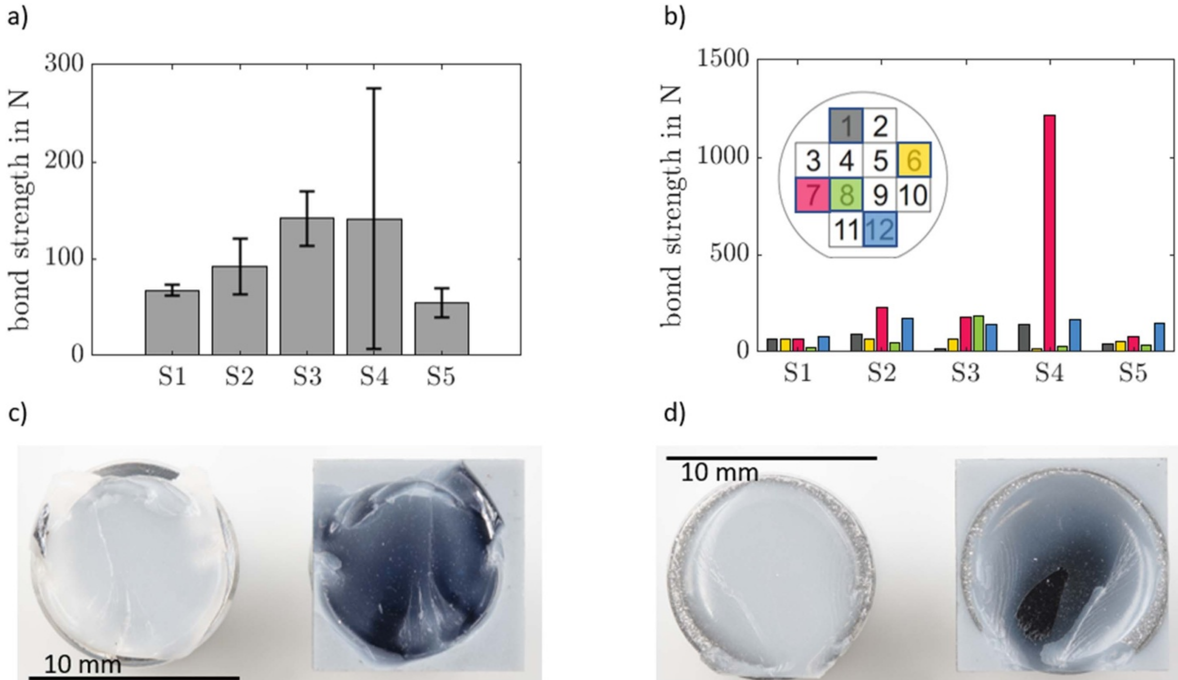

Figure 5. (a) Median of the bond strength and average deviation from median indicated as error bars. (b) Bond strength of the different sample positions on the sintered substrate. (c) Fracture pattern for substrate S3 position 7 with a bond strength of 179 N. The resulting ceramic part of the sample is shown on the left side, while the silicon side covered with rests of ceramic is shown on the right side. (d) Fracture pattern for substrate S4 position 7 with a bond strength of 1218 N.

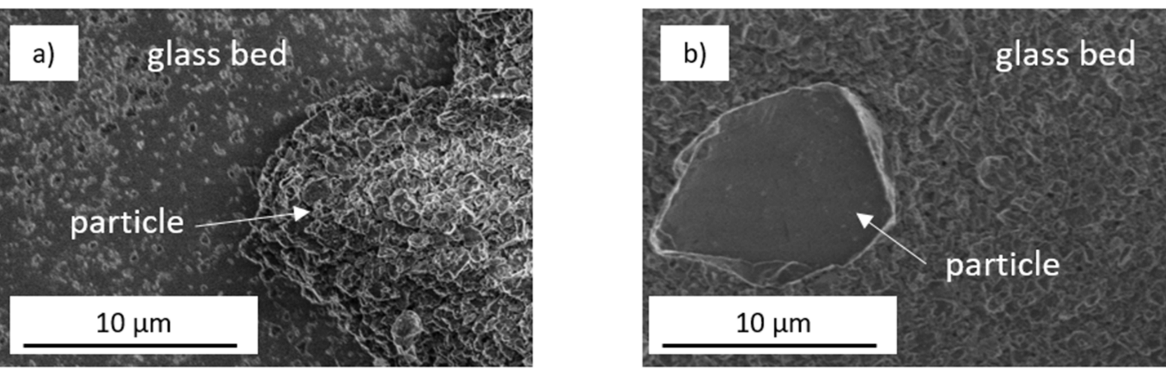

Figure 6. (a) SEM image of the LTCC side of substrate S6 that was sintered at temperatures up to 550 °C. A non-molten particle with a rough surface is placed on a partly molten glass bed. (b) SEM image of the LTCC side of substrate S7 that was sintered at temperatures up to 730 °C. A molten particle with a smooth surface is observed on a molten glass bed.

The median bond strength with average deviation is shown in figure 5(a) whilst figure 5(b) shows the bond strengths for the different sample positions. Despite of the variations in the measured bond strengths, the fracture patterns (see figures 5(c) and (d)) look comparable for high and low measured bond strengths. It should be noted that the samples do not tear at the interface, but mainly in the ceramic material. From the sintering experiments focussed on the impact of wetting layers and the sintering pressure (substrates S1–S5), no influences on the bonding result could be identified. All sintered substrates share a comparable optical appearance and bonding homogeneity. The observed differences in the bond strength could therefore, neither be explained with respect to the sonographic scans nor to the fracture patterns of the samples. The SiCer substrates S6 and S7, which were sintered at temperatures of 550 °C and 730 °C, showed an adequate bonding between LTCC, TiO_2 wetting layer and silicon. A difference between sintering at these temperatures compared to sintering at 900 °C is the compression grade of the LTCC. Thus, gluing of the samples to the aluminum sample holders was not possible and therefore no measurements of the bond strength could be conducted. Scanning electron microscope images illustrate the different melting behavior of glass particles due to glass transition temperatures of the LTCC glass components (see figures 6(a) and (b)). These particles are part of the LTCC matrix of the specimens used and can be observed at the LTCC side of the

SiCer samples. For substrate S6, glass particles can be identified that are not molten, whereas for S7 the particles are molten and embedded in a glass melt.

The thermal stress induced bowing of the sintered substrates was measured (MicroProf® TTV, FRT Metrology, Bergisch Gladbach, Germany). Comparing sample S1 and S2, sintered at 900 °C peak temperature and with a TiO_2 intermediate layer, the bow is 17 μm and 16 μm, respectively. The difference in applied pressure seems to have no significant influence on the resulting bow. Without TiO_2 interface layer, the bow value increases when a lower pressure is applied. S4 shows a bow of 13 μm while sample S5 exhibits a bow value of 21 μm, which indicates a potential stress reduction caused by the TiO_2 layer. Substrate S3 with oblique angle deposited Ti has a bow value of 18 μm, which is in comparable range to S1 and S2. Notably, the substrates that were sintered at lower temperatures have lower bow values of 4.2 μm (S6) and 8.3 μm (S7). This behavior can be explained by the lower grade of compression of the LTCC.

5. Conclusion

In this paper, the fabrication process for SiCer substrates is investigated with respect to the thermal behavior of the green LTCC, the influence of a wetting promoting TiO_2 layer between silicon and LTCC, the sintering temperature profile and the sintering pressure on the bonding result of SiCer compound substrates. From the results, no distinct influence of the different parameters was observed. Even at lower sintering temperatures, bonding-like adhesive forces between LTCC and silicon were observed. TGA measurements showed the outgassing of solvents and decomposition of binders, which could be correlated with the mass loss of the DSC measurements. From the DSC measurements of unlaminated and laminated LTCC, a shift in the endothermic peaks could be identified as well as a shift in mass loss for the TGA. The first significant drop in the mass loss observed between 200 °C and 280 °C shows only slight differences between laminated and unlaminated material. The second significant mass loss observed between 280 °C and 400 °C for the laminated material and 280 °C and 420 °C for the unlaminated material is slightly shifted to lower temperatures for the laminated material. While the mass loss for the unlaminated material terminates at around 500 °C the laminated material shows a further mass loss up to a temperature of 600 °C but of only about 1%, which was attributed to a thermal decomposition of the organic materials. Therefore, lamination processes using a pressure of 21 MPa at 82 °C affect the thermal behavior of LTCC in the temperature range of 300 °C–350 °C. In this temperature regime, the endothermic processes and the outgassing of the second component of the contained binder leads to a decrease in the thermal diffusivity of the laminated LTCC material measured by LFA. Thus, it can be concluded that the pre-processing of the green ceramic is a critical step in the entire SiCer fabrication flow that can influence the thermal behavior during sintering.

Data availability statement

The data that support the findings of this study are available upon reasonable request from the authors.

Acknowledgments

The authors gratefully acknowledge financial support by the BMBF (Grant 03WKDG01J). We thank furthermore M Schlosser from the Plastics Technology Group at Technische Universität Ilmenau for the possibility of conducting the pulling tests. Support by the Center of Micro- and Nanotechnologies (ZMN) of the TU Ilmenau, is gratefully acknowledged. We thank B Weidenfeller and M Dröttboom from Technische Universität Clausthal for the possibility to conduct DSC, LFA and TGA measurements. At least, we thank Paul Bucklitsch from Microsystems Technology Group at Technische Universität Ilmenau for the technical support and the bow measurements.

ORCID iDs

Laura Mohr-Weidenfeller https://orcid.org/0000-0002-8805-7268
Steffen Strehle https://orcid.org/0000-0002-1261-2894

References

[1] Glück M 2005 *MEMS in der Mikrosystemtechnik* (Wiesbaden: Vieweg Teubner Verlag)
[2] Fischer M *et al* 2015 RF-MEMS-platform based on silicon-ceramic-composite-substrates *2015 German Microwave Conf.* (IEEE) pp 398–401
[3] Fischer M, Gropp S, Stegner J, Frank A, Hoffmann M and Mueller J 2019 Silicon-ceramic composite substrate: a promising RF platform for heterogeneous integration *IEEE Microw. Mag.* **20** 28–43
[4] Torres D E *et al* 2008 A new method for wafer level integration of silicon components on LTCC *2nd European Conf. & Exhibition on Integration Issues of Miniaturized Systems-MOMS, MOEMS, ICS and Electronic Components* (VDE) pp 1–3
[5] Fischer M *et al* 2012 SiCer-A substrate to combine ceramic and silicon based micro systems *Additional Papers and Presentations, 2012* pp 000158–61
[6] Gropp S *et al* 2016 Wetting behaviour of LTCC and glasses on nanostructured silicon surfaces during sintering *Micro-Nano-Integration; 6. GMM-Workshop* (VDE) pp 1–5
[7] Gropp S *et al* 2016 Fabrication of an RF-MEMS-switch on a hybrid Si-ceramic substrate *Additional Papers and Presentations, 2016* pp 000118–21
[8] Wenzel R N 1936 Resistance of solid surfaces to wetting by water *Ind. Eng. Chem.* **28** 988–94
[9] Karabacak T, Picu C R, Senkevich J J, Wang G-C and Lu T-M 2004 Stress reduction in tungsten films using nanostructured compliant layers *J. Appl. Phys.* **96** 5740–6
[10] Barranco A *et al* 2016 Perspectives on oblique angle deposition of thin films: from fundamentals to devices *Prog. Mater. Sci.* **76** 59–153
[11] Institut für Arbeitsschitz der Deutschen Gesetzlichen Unfallversicherung *GESTIS-Stoffdatenbank*

(available at: https://gestis.dguv.de/data?name=010070) (Accessed 31 March 2022)

[12] Institut für Arbeitsschitz der Deutschen Gesetzlichen Unfallversicherung *GESTIS-Stoffdatenbank* (available at: https://gestis.dguv.de/data?name=012660) (Accessed 31 March 2022)

[13] Motlatle A M *et al* 2020 The thermal degradation kinetics and morphology of poly (vinyl butyral) cast films prepared using different organic solvents *AIP Conf. Proc.* **2289** 020071

[14] Dhaliwal A K and Hay J N 2002 The characterization of polyvinyl butyral by thermal analysis *Thermochim. Acta* **391** 245–55

[15] Cowan R D 1963 Pulse method of measuring thermal diffusivity at high temperatures *J. Appl. Phys.* **34** 926–7

[16] Weidenfeller B, Rode H, Weidenfeller L and Weidenfeller K 2020 Crystallinity, thermal diffusivity, and electrical conductivity of carbon black filled polyamide 46 *J. Appl. Polym. Sci.* **137** 48882

[17] Salazar A 2003 On thermal diffusivity *Eur. J. Phys.* **24** 351

[18] Enríquez E, Fuertes V, Cabrera M J, Seores J, Muñoz D and Fernández J F 2017 New strategy to mitigate urban heat island effect: energy saving by combining high albedo and low thermal diffusivity in glass ceramic materials *Sol. Energy* **149** 114–24

[19] Moskal G, Mikuśkiewicz M and Jasik A 2019 Thermal diffusivity measurement of ceramic materials used in spraying of TBC systems *J. Therm. Anal. Calorim.* **138** 4261–9